

## Supporting Information

### **In-situ polymerized synthesis of MnO nanoparticles anchored on N, S co-doped carbon as efficient cathodes for quasi-solid-state zinc ion battery**

Linpo Li<sup>1,\*</sup>, Yingchao Wang<sup>1</sup>, Gang Jiang<sup>1</sup>, Jing Li<sup>2</sup>, Mingyu Wang<sup>3</sup>, Yanli Niu<sup>1</sup>,

<sup>\*</sup>, Enbo Shangguan<sup>1,2,3\*</sup>

*<sup>1</sup>Henan Engineering Research Center of Design and Recycle for Advanced Electrochemical Energy Storage Materials, School of Materials Science and Engineering, Henan Normal University, Xinxiang 453007, PR China*

*<sup>2</sup>Collaborative Innovation Center of Henan Province for Green Manufacturing of Fine Chemicals, Key Laboratory of Green Chemical Media and Reactions Ministry of Education, School of Chemistry and Chemical Engineering, Henan Normal University, Xinxiang 453007, PR China*

*<sup>3</sup>Henan Chaoli New Energy Co., Ltd, Xinxiang 453007, P.R. China*

\* Corresponding author: **Linpo Li, Yanli Niu, Enbo Shangguan**

Email: [lilinpo@htu.edu.cn](mailto:lilinpo@htu.edu.cn) (Linpo Li)

[niuyanli1992@163.com](mailto:niuyanli1992@163.com) (Yanli Niu)

[shangguanenbo@163.com](mailto:shangguanenbo@163.com) (Enbo Shangguan)

## **Experimental Section:**

All involved chemicals were purchased from Sigma-Aldrich Reagent Co. The reagents and solvents were of analytical grade and used without any extra purification.

### **Preparation of MnO@NSC hybrids**

Typically, 14.7 g (1 M)  $(\text{CH}_3\text{COO})_2\text{Mn}\cdot 4\text{H}_2\text{O}$ , 6 g AM monomer, 36 mg  $\text{C}_7\text{H}_{10}\text{N}_2\text{O}_2$  cross-linker and 90 mg  $\text{K}_2\text{S}_2\text{O}_8$  initiator were dispersed into 60 mL deionized water and stirred for 0.5 h at 40 °C to adequately dissolve. Next, the obtained mixture solution was poured into a sealed container glass bottle and heated in an electric oven at 60 °C for 4 h to in situ polymerization, forming uniform PAM-Mn hydrogel. Subsequently, the resulting hydrogel was dried at 60 °C in the oven for 20 h. Finally, the precursor was calcined at 800 °C for 2 h with a heating rate of 5 °C  $\text{min}^{-1}$  in  $\text{N}_2$  flowing to obtain core-shell MnO@NSC nanoparticles.

For comparison study, 7.35 g (0.5 M) and 22.06 g (1.5 M)  $(\text{CH}_3\text{COO})_2\text{Mn}\cdot 4\text{H}_2\text{O}$  were also selected as Mn sources to make MnO@NSC hybrids employing the above method.

### **Materials Characterization:**

The morphology of MnO@NSC samples is investigated by using field emission scanning electron microscopy (FESEM; SU8010, 10 kV) and transmission electron microscopy (TEM, JEM-2100, Japan). Energy-dispersive X-ray spectroscopy (EDS) was used to record elemental distribution. The compositions and structures of MnO@NSC hybrids were analyzed by XRD images (XRD, Bruker, Advance D8A), Raman spectroscopy (Witech. CRM200, 532 nm), and XPS (ESCALAB250Xi) images. The content of C was measured by adopting a TA/SDT650 thermal analyzer at 10 °C  $\text{min}^{-1}$  from 25 to 800 °C under air atmosphere. The specific surface area and the pore-size distribution of MnO@NSC samples is tested by automatic gas adsorption analyzer (Autosorb iQ). The Mn content in electrolyte after the initial CV charge scan was measured by the inductively coupled plasma-optical emission spectrometry (ICP-OES).

### **Electrochemical Performance Testing**

Cyclic voltammetry curves at 0.1, 0.2, 0.4, 0.6 mV s<sup>-1</sup> and electrochemical impedance spectroscopy (100 kHz to 0.1 Hz) were evaluated on electrochemical workstation (CHI 760D). All the galvanostatic charge/discharge tests were conducted on Neware CT-4008 battery test systems (Shenzhen, China) in the potential ranging from 0.8 to 1.9 V (vs. Zn/Zn<sup>2+</sup>). MnO@NSC electrode was prepared by uniformly mixing MnO@NSC active materials, carbon black conductive agents and polytetrafluoroethylene (PTFE) binders via grinding for 20 min to obtain a shiny electrode film, and then such film (area: 1 cm<sup>2</sup>) was pressed onto clean Ti mesh with a pressure of 10 MPa cm<sup>-2</sup> followed by drying in a oven at 100 °C for 16 h. AZIB was assembled by employing Zn foil (thickness: 10 μm) as a anode, MnO@NSC (mass loading: 2-3 mg) a cathode, 2 M ZnSO<sub>4</sub>·7H<sub>2</sub>O + 0.2 M MnSO<sub>4</sub>·H<sub>2</sub>O as an electrolyte and glass fiber separator (GF/D, Whatman) as a separator. The quasi-solid-state ZIB was further assembled by using PAM-based hydrogel instead of the above liquid electrolyte and glass fiber separator. The synthetic methods of hydrogel are as follows: 28.75 g of ZnSO<sub>4</sub>·7H<sub>2</sub>O, 1.69 g of MnSO<sub>4</sub>·H<sub>2</sub>O, 5 g AM monomer, 15 mg C<sub>7</sub>H<sub>10</sub>N<sub>2</sub>O<sub>2</sub> cross-linker and 75 mg K<sub>2</sub>S<sub>2</sub>O<sub>8</sub> initiator were dissolved into 50 mL deionized water, held at 40 °C to fully dissolve. Then, the homogenous solution was transferred into a mold and maintained at 60 °C for 4 h to get a brownish red PAM-based hydrogel.

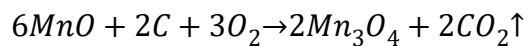
Energy and power densities ( $E$  and  $P$ ) of such AZIB were evaluated based on the calculation formulas of

$$E = \int_0^{\Delta t} IV(t) dt / m$$

$$P = E/\Delta t$$

where  $I$  refers to discharging current (A),  $V(t)$  represents discharging voltage at  $t$  (V),  $dt$  and  $\Delta t$  is time differential and discharging time (s), respectively,  $m$  is mass of MnO

The total MnO content in final sample can be estimated by TGA analysis toward MnO@C. The corresponding reaction equation for MnO@C in air atmospheres is shown below:



According to the mass for annealed products of MnO@C and molar ratio relationships in between  $Mn_3O_4$ , we can calculate the MnO ( $M_1$ ) content in MnO@NSC. The calculation details are listed as follows:

$$\frac{\frac{M_1 \times 0.8044}{228.81} \times 3 \times 70.938}{M_1} = 0.748$$

Therefore, the mass percent concentration of MnO in the MnO@C sample is calculated to be ~74.8%.

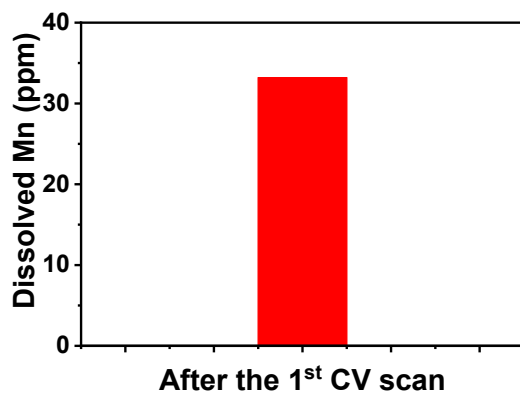


**Fig. S1** Content of  $Mn^{2+}$  in 2 M  $ZnSO_4$  electrolytes after the initial CV charge scan

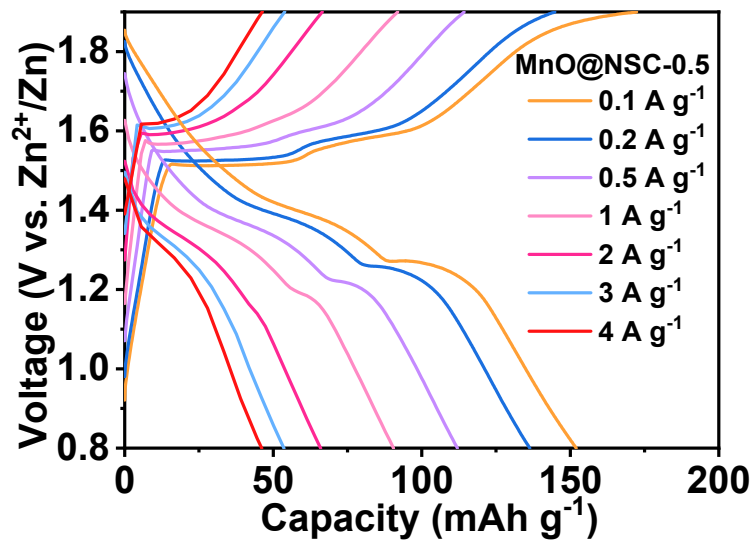


Fig. S2 GCD curves of MnO@NSC-0.5

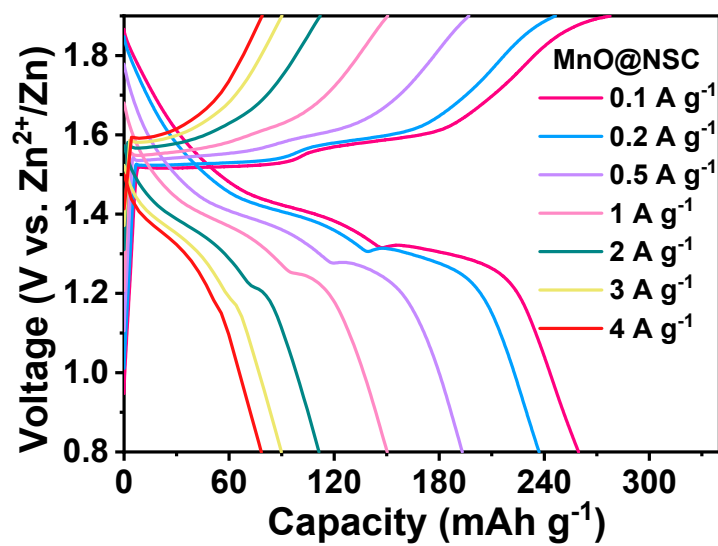


Fig. S3 GCD curves of MnO@NSC

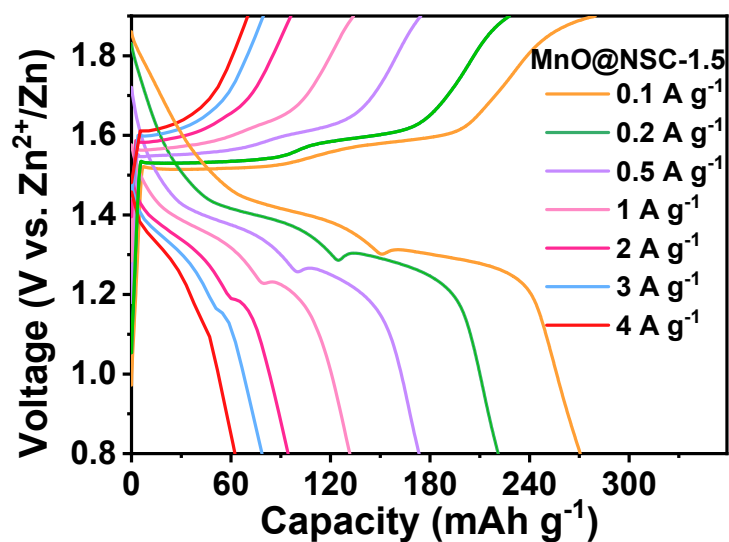


Fig. S4 GCD curves of MnO@NSC-1.5

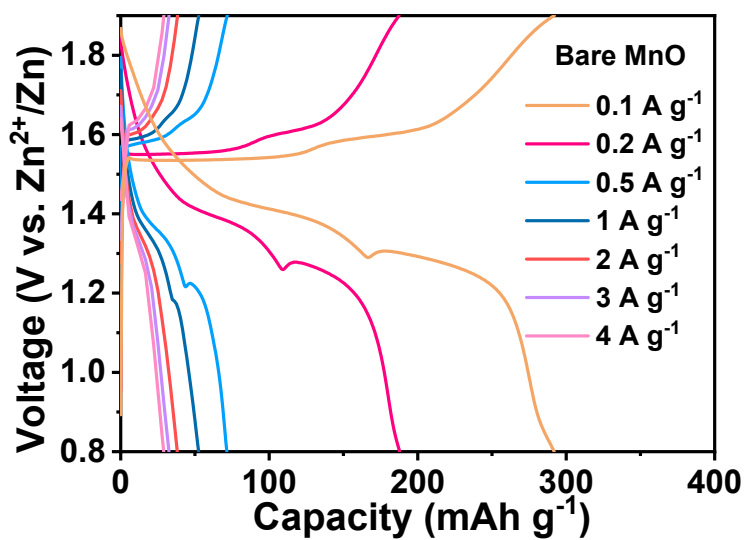


Fig. S5 GCD curves of bare MnO

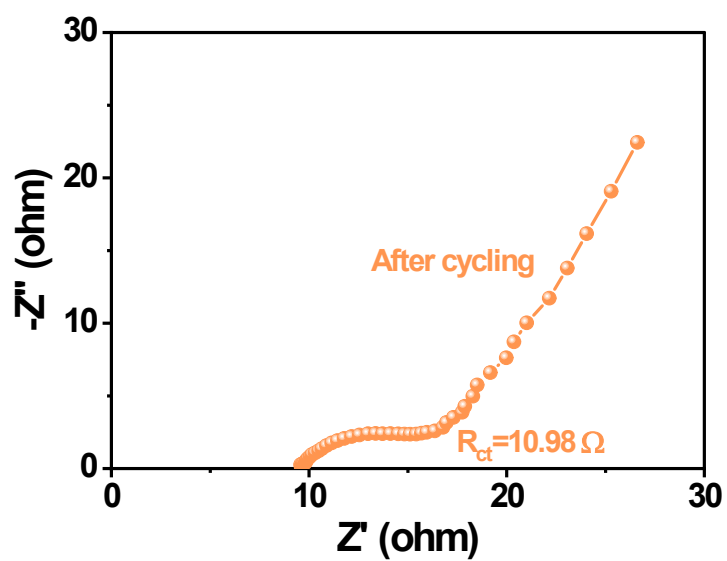


Fig. S6 Nyquist plot of cycled MnO@NSC electrode

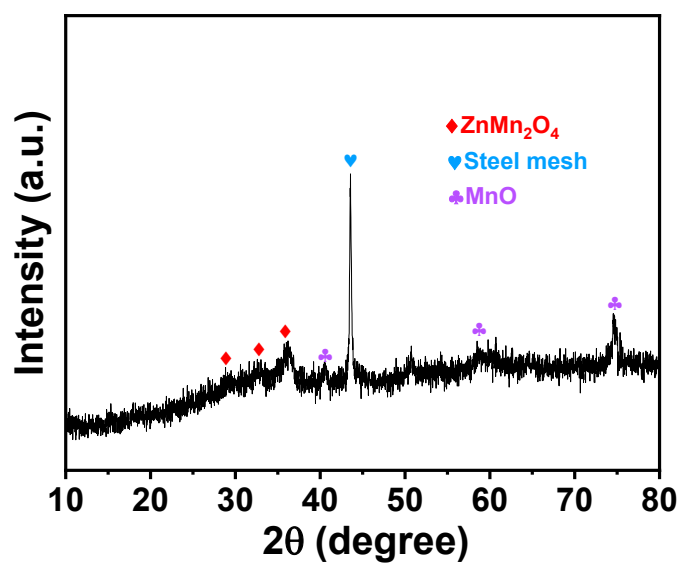


Fig. S7 XRD pattern of the cycled cathode

**Table S1** Cyclic performance comparison

Electrode	Remained Capacity (mAh g <sup>-1</sup> )	Mass loading (mg cm <sup>-2</sup> )	Ref.
MnO@NSC	139.75 at 2 A g <sup>-1</sup> after 5000 cycles	3	This work
$\alpha$ -Mn <sub>2</sub> O <sub>3</sub>	82.2 at 2 A g <sup>-1</sup> after 1000 cycles	-	[1]
CoMn-PBA	57.3 at 1 A g <sup>-1</sup> after 1000 cycles	-	[2]
N-VO-MnO <sub>1-x</sub>	135 at 0.5 A g <sup>-1</sup> after 600 cycles	1	[3]
MnO	10.5 at 0.5 A g <sup>-1</sup> after 600 cycles	1	[4]
MgMn <sub>2</sub> O <sub>4</sub>	96.8 at 0.5 A g <sup>-1</sup> after 500 cycles	-	[5]
MnO@NGS	112.3 at 0.5 A g <sup>-1</sup> after 300 cycles	-	[6]
Mn <sub>3</sub> O <sub>4</sub>	124 at 0.5 A g <sup>-1</sup> after 300 cycles	-	[7]
ZnMn <sub>2</sub> O <sub>4</sub> /C	84.6 at 0.5 A g <sup>-1</sup> after 500 cycles	2	[8]
MnO@C	102.9 at 1.5 A g <sup>-1</sup> after 1200 cycles	1.2	[9]
Cu-MnO <sub>2</sub>	111 at 5 A g <sup>-1</sup> after 700 cycles	1.5	[10]
MnO	103 at 1 A g <sup>-1</sup> after 1000 cycles	1.5	[11]
V <sub>2</sub> O <sub>5</sub>	36 at 10 A g <sup>-1</sup> after 1000 cycles	2.8	[12]
Zn <sub>x</sub> MnO <sub>2</sub> /CNT	101 at 3 A g <sup>-1</sup> after 2000 cycles	1	[13]
s			
MnO@N-C	95.3 at 0.5 A g <sup>-1</sup> after 200cycles	2	[14]
MnO <sub>2</sub>	131 at 0.5 A g <sup>-1</sup> after 400 cycles	2	[15]
MnO@C	56.5 at 2 A g <sup>-1</sup> after 1000 cycles	1	[16]

## References:

1. B. Jiang, C. Xu, C. Wu, L. Dong, J. Li, F. Kang, Manganese sesquioxide as cathode material for multivalent zinc ion battery with high capacity and long cycle life, *Electrochim. Acta*, 2017, **229**, 422-428.
2. Y. Zeng, X. Lu, S. Zhang, D. Luan, S. Li, X. Lou, Construction of Co-Mn prussian blue analog hollow spheres for efficient aqueous zn-ion batteries, *Angew. Chem. Int. Ed.*, 2021, **60**, 22189-22194.
3. P. Yu, J. Zhou, M. Zheng, M. Li, H. Hu, Y. Xiao, Y. Liu, Y. Liang, Boosting zinc ion energy storage capability of inert MnO cathode by defect engineering, *J. Colloid Interface Sci.*, 2021, **594**, 540-549.
4. C. Zhu, G. Fang, S. Liang, Z. Chen, Z. Wang, J. Ma, H. Wang, B. Tang, X. Zheng, J. Zhou, Electrochemically induced cationic defect in MnO intercalation cathode for aqueous zinc-ion battery, *Energy Storage Mater.*, 2020, **24**, 394-401.
5. V. Soundharajan, B. Sambandam, S. Kim, V. Mathew, J. Jo, S. Kim, J. Lee, S. Islam, K. Kim, Y.K. Sun, J. Kim, Aqueous magnesium zinc hybrid battery: an advanced high-voltage and high-energy  $MgMn_2O_4$  cathode, *ACS Energy Lett.*, 2018, **3**, 1998-2004.
6. W. Li, X. Gao, Z. Chen, R. Guo, G. Zou, H. Hou, W. Deng, X. Ji, J. Zhao, Electrochemically activated MnO cathodes for high performance aqueous zinc-ion battery, *Chem. Eng. J.*, 2020, **402**, 125509.
7. J. Hao, J. Mou, J. Zhang, L. Dong, W. Liu, C. Xu, F. Kang, Electrochemically induced spinel-layered phase transition of  $Mn_3O_4$  in high performance neutral aqueous rechargeable zinc battery, *Electrochim. Acta*, 2018, **259**, 170-178.
8. N. Zhang, F. Cheng, Y. Liu, Q. Zhao, K. Lei, C. Chen, X. Liu, J. Chen, Cation-deficient spinel  $ZnMn_2O_4$  cathode in  $Zn(CF_3SO_3)_2$  electrolyte for rechargeable aqueous zn-ion battery, *J. Am. Chem. Soc.*, 2016, **138**, 12894-12901.
9. R. Zhang, Q. Ma, S. Chen, J. Huang, L. Zhu, J. Liu, Reaction mechanism and electrochemical performance of manganese (II) oxide in zinc ion batteries, *Solid State Ion.*, 2020, **356**, 115439.
10. R. Zhang, P. Liang, H. Yang, H. Min, M. Niu, S. Jin, Y. Jiang, Z. Pan, J. Yan, X.

- Shen, J. Wang, Manipulating intercalation-extraction mechanisms in structurally modulated  $\delta$ -MnO<sub>2</sub> nanowires for high-performance aqueous zinc-ion batteries, *Chem. Eng. J.*, 2022, **433**, 133687.
11. Z. You, H. Liu, J. Wang, L. Ren, J.-G. Wang, Activation of MnO hexagonal nanoplates via in situ electrochemical charging toward high-capacity and durable Zn-ion batteries, *Appl. Surface Sci.*, 2020, **514**, 145949.
  12. Y. Yang, Y. Tang, G. Fang, L. Shan, J. Guo, W. Zhang, C. Wang, L. Wang, J. Zhou, S. Liang, Li<sup>+</sup> intercalated V<sub>2</sub>O<sub>5</sub>·nH<sub>2</sub>O with enlarged layer spacing and fast ion diffusion as an aqueous zinc-ion battery cathode, *Energy Environ. Sci.*, 2018, **11**, 3157-3162.
  13. F. Jing, J. Pei, Y. Zhou, Y. Shang, S. Yao, S. Liu, G. Chen, High-performance reversible aqueous zinc-ion battery based on Zn<sup>2+</sup> pre-intercalation alpha-manganese dioxide nanowires/carbon nanotubes, *J. Colloid Interface Sci.*, 2022, **609**, 557-565.
  14. F. Tang, T. He, H. Zhang, X. Wu, Y. Li, F. Long, Y. Xiang, L. Zhu, J. Wu, X. Wu, The MnO@N-doped carbon composite derived from electrospinning as cathode material for aqueous zinc ion battery, *J. Electroanal. Chem.*, 2020, **873**, 114368.
  15. J. Zhai, J. Yan, G. Wang, S. Chen, D. Jin, H. Zhang, W. Zhao, Z. Zhang, W. Huang, Surface modification of manganese monoxide through chemical vapor deposition to attain high energy storage performance for aqueous zinc-ion batteries, *J. Colloid Interface Sci.*, 2021, **601**, 617-625.
  16. S. Li, D. Yu, L. Liu, S. Yao, X. Wang, X. Jin, D. Zhang, F. Du, In-situ electrochemical induced artificial solid electrolyte interphase for MnO@C nanocomposite enabling long-lived aqueous zinc-ion batteries, *Chem. Eng. J.*, 2022, **430**, 132673.